NJC

Accepted Manuscript

This article can be cited before page numbers have been issued, to do this please use: J. Stejskal, P. Bober, M. Trchova, J. Horsky, Z. Walterova, S. K. Filippov, T. Plachy and M. Mrlík, *New J. Chem.*, 2018, DOI: 10.1039/C8NJ01283K.

ROYAL SOCIETY OF CHEMISTRY

rsc.li/njc

View Article Online
DOI: 10.1039/C8NJ01283K

Oxidation of pyrrole with *p*-benzoquinone to semiconducting products and their application in electrorheology

Jaroslav Stejskal,[*a] Patrycja Bober,[a] Miroslava Trchová,[a] Jiří Horský,[a] Zuzana Walterová,[a] Sergey K. Filippov,[a] Tomáš Plachý,[b] Miroslav Mrlík[b]

[a] *Institute of Macromolecular Chemistry Academy of Sciences of the Czech Republic, 162 06 Prague 6, Czech Republic*

[b] *Centre of Polymer Systems, Tomas Bata University in Zlin, 760 01 Zlin, Czech Republic*

***Corresponding author:**

E-mail: stejskal@imc.cas.cz

ABSTRACT: Low-molecular-weight organic semiconducting material was prepared by the redox interaction between pyrrole and *p*-benzoquinone. The reaction between pyrrole and *p*-benzoquinone in aqueous solutions of methanesulfonic acid proceeded smoothly at room temperature. The product with a globular morphology obtained in high yield in 0.1 M methanesulfonic acid had the highest conductivity, 4.6×10^{-6} S cm^{-1}. On the other hand, the samples prepared in the absence of acid or at its high concentration were non-conducting. EPR spectroscopy confirmed the presence of electronic species as charge carriers responsible for conductivity. Dominating component was proved to be a low-molecular-weight adduct composed of quinhydrone complex and pyrrole molecule. FTIR and Raman spectra were used to discuss molecular structure in detail. Strong electrorheological effect with very fast response time was demonstrated by reproducible increase in the viscosity of suspensions in silicone oil after application of electric field. The effect is discussed with the help of dielectric spectroscopy.

Keywords: Pyrrole; *p*-Benzoquinone; Oxidation; Conductivity; FTIR and Raman spectroscopies; Electrorheology

View Article Online
DOI: 10.1039/C8NJ01283K

Introduction

Polypyrrole, an important conducting polymer, is usually prepared by the oxidation of pyrrole with iron(III) chloride[1,2] or ammonium peroxydisulfate.[3] In attempt to prepare this polymer with organic oxidant, *p*-benzoquinone, electroactive products have been obtained[4] but their polymeric character was not confirmed. The present study suggests that oxidation products are indeed of low-molecular-weight nature but conducting, and thus of potential interest. The polymerization route has been replaced by the covalent substitution of *p*-benzoquinone with pyrrole. Early study assumed the coupling of two *p*-benzoquinone molecules with pyrrole in *β*-position.[5] (**1**) (Fig. 1). Later report proposed the substitution of *p*-benzoquinone with two pyrroles in α-positions[6] (**2**) and, based on the spectroscopic study, the coupling involving nitrogen atoms was excluded.

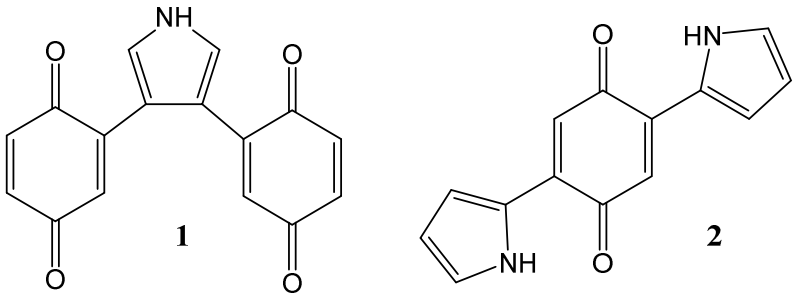

Fig. 1. The proposed compounds produced by the reaction of pyrrole and *p*-benzoquinone.

The redox reaction between pyrrole and *p*-benzoquinone is a special case of the substitution of *p*-benzoquinone ring with nitrogen containing compounds, such as aniline,[7,8] *p*-phenylenediamine,[9–11] benzimidazole,[12] imidazole[12,13], and others.[7] Please note that hydrogen atoms abstracted during the substitution from *p*-benzoquinone ring may also be added to oxygen atoms in the same molecule, and *p*-benzoquinone moiety converts to hydroquinone one. For that reason, the substitution is also regarded as an addition reaction, and its products as adducts. Especially *p*-benzoquinone substituted with one or two nitrogen-containing molecules, such as **2**, have been considered most frequently in the literature.
[7,14] Opinions still differ whether the bonding to *p*-benzoquinone involves nitrogen atoms[7–16] or not.[6,17,18] The former hypothesis, however, has been preferred, especially on account of the analogous reactions of *p*-benzoquinone with aniline.[8]

View Article Online
DOI: 10.1039/C8NJ01283K

Some products displayed the conductivity up to 10^{-4} S cm^{-1} [8, 9], and could be applicable in energy-storage devices[18] or in electrorheology.[10] Their electroactivity[4] may be of interest in corrosion protection in the combination with good adhesion to metals.[14] The present study concentrated on the reaction between pyrrole with *p*-benzoquinone under various acidity conditions, and on the characterization of the products with respect to their structure and conductivity. The application in electrorheology, where the rheology of suspensions is controlled by electric field[19,20] and conducting polymers had often been applied,[21,22] has been tested in the next step.

Experimental

Preparation

p-Benzoquinone (3.24 g, 30 mmol) was dissolved in the aqueous solution of methanesulfonic acid (MSA), pyrrole was added (1.34 g, 20 mmol) and the volume was adjusted to 100 mL. The concentration of MSA was varied from 0 to 10 M in the individual experiments. MSA was used for the acidity control because it does not precipitate silver ions, which may be benefit in potential preparation of composites with silver.[23] The yellowish reaction mixture darkened and brown-to-black precipitate appeared within tens of minutes. The reaction was left to proceed for 3 days at room temperature, the mixture being occasionally briefly shaken. The solids then were collected by filtration, rinsed first with the corresponding acid solution, then with ethanol, and dried in the open air.

Spectroscopy

Infrared spectra were recorded using a Thermo Nicolet NEXUS 870 FTIR Spectrometer (DTGS TEC detector; 64 scans; resolution 2 cm^{-1}) in transmission mode after dispersion of samples in potassium bromide pellets. The spectra were corrected for the carbon dioxide and humidity in the optical path. Raman spectra were recorded with a Renishaw InVia Reflex Raman microspectrometer. The spectra were excited with a near infrared diode 785 nm laser. A research-grade Leica DM LM microscope with an objective magnification ×50 was used to focus the laser beam on the sample placed on an X–Y motorized sample stage. The scattered light was analysed with a spectrograph using a holographic grating 1200 lines mm^{-1}. A Peltier-cooled CCD detector (576×384 pixels) registered the dispersed light.

View Article Online
DOI: 10.1039/C8NJ01283K

Conductivity

The conductivity was determined by a van der Pauw method on powders compressed to pellets (diameter 13 mm, thickness 1.0 ± 0.2 mm) under pressure 530 MPa with a hydraulic press Trystom H-62 (Trystom, Czech Republic). A Keithley 230 Programmable Voltage Source in serial connection with a Keithley 196 System DMM was used as a current source, the potential difference between the potential probes was measured with a Keithley 181 Nanovoltmeter (Keithley, USA).

Mass spectrometry

Solvent-free laser desorption ionization mass spectrometry (LDI-MS) was used.[24] The powdered sample prepared in 0.1 M MSA was transferred without any matrix or ionization agent added to a ground-steel target plate with a disposable tip and gently pressed to a thin film. Loose grains were wiped off. MS spectra were obtained with a ultrafleXtreme TOF-TOF mass spectrometer (Bruker Daltonics) equipped with a 2000 Hz smartbeam-II laser (355 nm) using the positive-ion reflectron mode and panoramic pulsed ion extraction. The values of *M*/z were assigned using the external calibration with poly(ethylene glycol) 600.

Electron paramagnetic resonance

Measurements have been performed at room temperature using a Bruker ELEXSYS E-540 X-band spectrometer at microwave power output 6 mW and 100 kHz magnetic modulation of amplitudes 0.1 G with the samples placed in a quartz tube of outer diameter 3 mm. At least three independent experiments were performed per each sample and the error of spin-concentration determination and the results were averaged.

Electrorheology

Dried particles doped with 0.1 M MSA were mixed with a silicone oil (Lukosiol M200, Chemical Works Kolín, Czech Republic, viscosity $\eta_c = 194$ mPa s, conductivity $\sigma_c \approx 10^{-11}$ S cm^{-1}) in a ratio 1:9 (w/w) in order to create a novel electrorheological fluid. Electrorheological measurements were performed at shear rates 0.01–250 s^{-1} and 25 °C using a rotational rheometer (Bohlin Gemini, UK) with a plate-plate geometry of a diameter 20 mm. An external electric field in a perpendicular direction to the shearing was supplied by a DC high-voltage supplier TREK 668B (TREK, USA). Electric field was applied 1 min before shearing in order to provide time enough for the particles to create organized structures. Internal chain-like structures formed by particles upon an application of external electric field

View Article Online
DOI: 10.1039/C8NJ01283K

were revealed with an optical microscope (Leica DVM2500; Leica Microsystems, UK). A suspension consisting of 1 wt% was placed on the glass between two copper electrodes with a gap 1 mm, and an electric field of strength 0.5 kV mm^{-1} was supplied by a DC high-voltage source (Keithley 2400, USA).

Dielectric spectroscopy

Dielectric measurements were carried out with an impedance dielectric spectroscopy analyzer, Novocontrol Concept 50 (Novocontrol, Germany) in a frequency range from 0.5 Hz to 2 MHz. They dielectric spectra were analysed using the Havriliak-Negami (H-N) model.[25]

Results and discussion

The present study was motivated by the preparation of conducting polymer, polypyrrole, by using an original organic oxidant of pyrrole, *p*-benzoquinone, instead of classical inorganic oxidants, such as iron(III) salts[1,2,26] or peroxydisulfate.[3] The oxidation products with moderate conductivity have indeed been obtained depending on the acidity of reaction medium using the solutions of MSA but the chemistry of pyrrole oxidation turned to be more complex as discussed below.

Morphology

The spherical particle were produced when the oxidation of pyrrole took place in aqueous medium in the absence of acid and converted to globular morphology as the concentration of acid increased (Fig. 2). The similar trend has been reported for the oxidation of aniline.[27] Under neutral conditions, the miscibility of both aniline and pyrrole with water is limited and they tend to produce monomer droplets that are subsequently converted to solid spheres. After the acidity of the reaction medium increases, both monomers become protonated and well soluble, the precipitation polymerization affords irregular globules. The size of aggregates may vary depending on the nucleation and generation rates.

View Article Online
DOI: 10.1039/C8NJ01283K

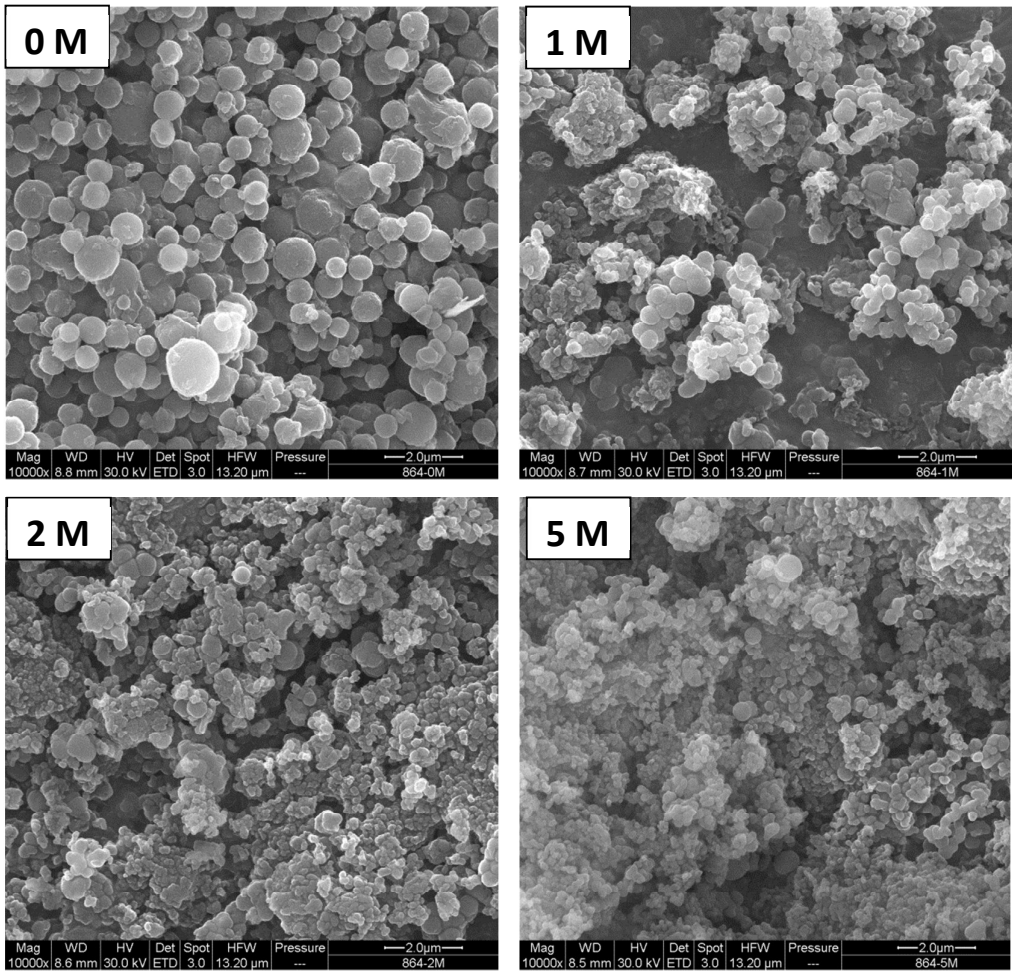

Fig. 2. Scanning electron micrographs of the samples prepared at various molar concentration of MSA. Scale bar 2 μm.

Conductivity

The conductivity of reaction products is of prime interest for applications based on electrical properties of materials. When pyrrole was oxidized in the solutions of MSA of various molar concentrations, the conducting products have been obtained in most cases (Table 1, Fig. 3). The product prepared in the absence of MSA, however, was non-conducting (Table 1). The increasing concentration of MSA improved the conductivity to up to 4.60×10^{-6} S cm^{-1} at 0.1 M MSA (Fig. 3) and it decreased at higher MSA concentrations (Table 1). The conductivity fell below 10^{-11} S cm^{-1} for the preparation in 10 M MSA.

View Article Online
DOI: 10.1039/C8NJ01283K

Table 1. The yield, conductivity, spin concentration and elemental composition of the products of pyrrole oxidation with *p*-benzoquinone prepared in the solutions of methanesulfonic acid of various molar concentrations, [MSA].

[MSA], M	Yield, g g^{-1} pyrrole	Conductivity, S cm^{-1}	Spins, mol mg^{-1}	C, wt.%	H, wt.%	N, wt.%	O,S, wt.%
0	1.18	1.64×10^{-11}	8.8×10^{-10}	51.7	3.3	4.3	40.7
0.1	1.80	4.60×10^{-6}	7.9×10^{-7}	60.8	3.6	7.8	27.8
1	1.91	6.85×10^{-7}	6.0×10^{-6}	63.3	3.9	7.2	25.6
5	2.75	1.43×10^{-8}	3.1×10^{-8}	33.3	5.3	3.1	58.3

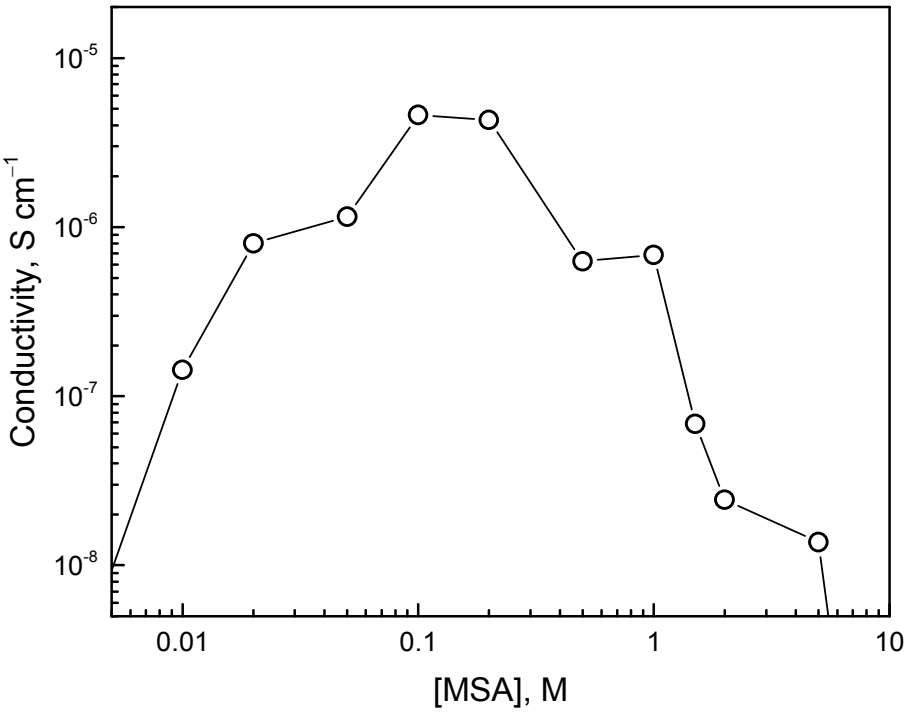

Fig. 3. Conductivity of products obtained at various molar concentrations of methanesulfonic acid in the reaction medium.

View Article Online
DOI: 10.1039/C8NJ01283K

EPR spectroscopy

EPR spectra clearly indicate the presence of unpaired electrons that manifested themselves in the spectrum as a singlet line (Fig. 4). The concentration of spins depends on the molar concentration of MSA (Table 1). The highest number of spins corresponds to the sample prepared in 1 M MSA. Interestingly, the line width of a singlet has also peculiarity at 1M of MSA showing the sharpest line in comparison with other MSA concentrations. The concentrations of the spins qualitatively correlate with the conductivity (Table 1). We therefore conclude that the conduction mechanism is of electronic nature, similarly like in conducting polymers.

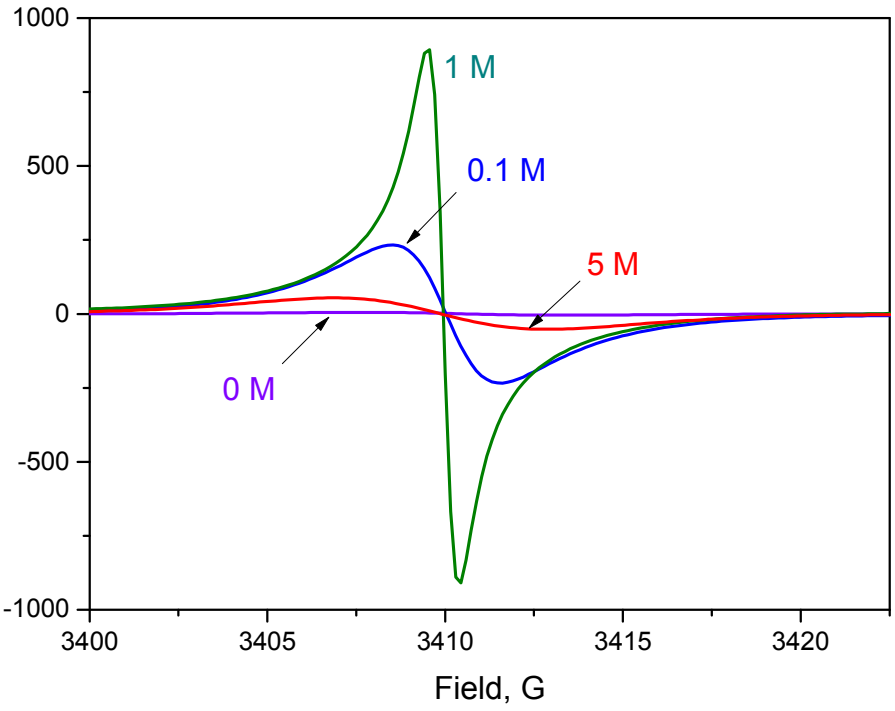

Fig. 4. EPR spectra of the samples prepared at various molar concentrations of methanesulfonic acid.

Mass spectrometry

In preliminary tests in gel permeation chromatography, no polymeric fraction has been detected in the samples dissolved in *N*-methylpyrrolidone. Polypyrrole thus was not produced. Mass spectrometry is probably the most efficient method for the analysis of reaction products composed of low-molecular-weight components. We have concentrated on the sample

View Article Online
DOI: 10.1039/C8NJ01283K

prepared in 0.1 M MSA (Fig. 5), which displayed the highest conductivity (Table 1). Most of the peaks were tentatively assigned by combining molecular weights of pyrrole, *p*-benzoquinone, and MSA as the most probable constituents. The difference between molecular weight observed in the spectrum and that of the assigned structure can be explained by the ionization type for 0 (loss of electron) and 1 (addition of proton). The difference of 2 can be explained by the reduction of one *p*-benzoquinone (plus 2 H) and ionization by the electron loss.

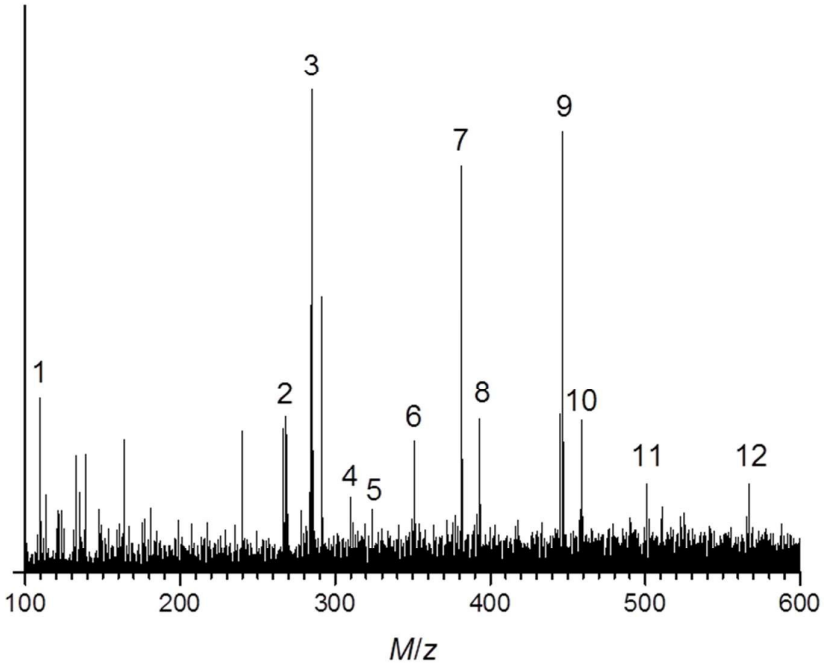

Fig. 5. Mass spectrum of the sample prepared in 0.1 M MSA. Numbers of above peaks correspond to those in Table 2. *M*/*z* is the mole mass-to-charge ratio of ions.

With exception of component 2 corresponding to a pyrrole tetramer, majority of products dominating the spectrum contains *p*-benzoquinone moieties in excess to the pyrrole. This is reflected by low content of nitrogen in samples revealed by elemental analysis (Table 1).

View Article Online
DOI: 10.1039/C8NJ01283K

Table 2. The assignment of the experimental mole mass-to-charge ratio of ions, *M*/*z*, to the theoretical molecular weight M_{theo} expected for compounds composed of various numbers of *p*-benzoquinone (BzQ) and pyrrole (Py) constitutional units and eventually methanesulfonic acid. Δ is the difference between experimental and assigned molecular weight.

Peak	*M*/*z*	M_{theo}	BzQ	Py	MSA	Δ	Formula
1	109.05	108.02	1	0	0	1	
2	268.29	268.17	0	4	0	0	
3	285.18	283.08	2	1	0	2	**3, 6**
4	310.18	309.15	1	3	0	1	
5	324.20	324.06	3	0	0	0	
6	351.21	350.13	2	2	0	1	
7	381.25	379.07	2	1	1	2	**4**
8	393.21	391.11	3	1	0	2	
9	446.27	446.11	2	2	1	0	
10	459.23	458.15	3	2	0	1	
11	501.22	499.13	4	1	0	2	
12	567.24	566.17	4	2	0	1	

The dominant product (3 in Fig. 5) is likely to be composed of two *p*-benzoquinone molecules and one pyrrole molecule, i.e. the structure (**1**) proposed already in 1911 by Mohlau and Redlich.[5] When we take into account the fact that the oxidation of pyrrole to polypyrrole takes place in *α*-positions,[1–3] the reaction to di-*α*,*α*'-(*p*-benzoquinone)pyrrole (**3**) is offered as more likely (Fig. 6):

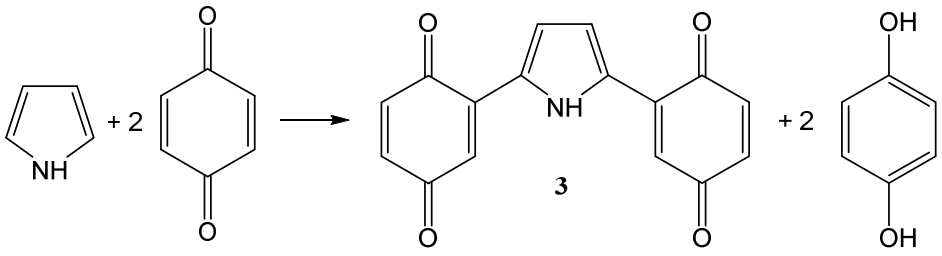

Fig. 6. The oxidation of pyrrole with *p*-benzoquinone is expected to yield mainly di-*α*,*α*'-(*p*-benzoquinone)pyrrole (**3**).

View Article Online
DOI: 10.1039/C8NJ01283K

The product **3** contains theoretically 68.3 wt% C, 3.9 wt% H, 5.0 wt% N and 22.7 wt.% O atoms. This is in qualitative agreement with the elemental analysis of the product prepared in 0.1 M MSA (Table 1) considering the presence of accompanying by-products.

The ability pyrrole and ring-substituted pyrroles to be protonated with strong acids was reported.[28] The compound **3** would produce a corresponding salt **4** (Fig. 7), which well corresponds to the component 7 in mass spectrum (Fig. 5, Table 2).

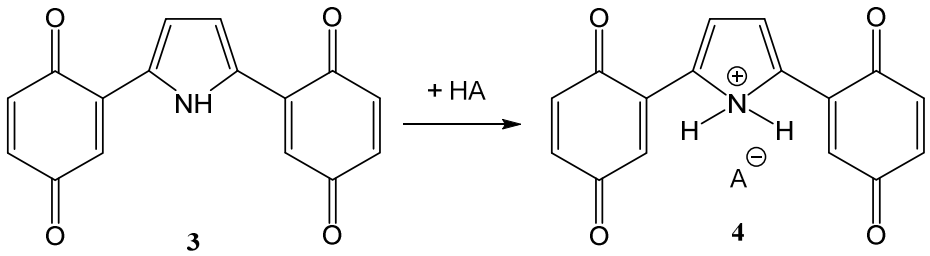

Fig. 7. The substituted pyrrole (**3**) is protonated with arbitrary acid HA, here methanesulfonic acid, to a corresponding salt (**4**).

Another process has still to be considered. It is well known that *p*-benzoquinone produces an equimolar charge-transfer complex with hydroquinone, quinhydrone, which is currently used in analytical electrodes. In present study, *p*-benzoquinone is reduced to hydroquinone (Fig. 6) and the formation of quinhydrone is possible. A compound composed of quinhydrone and pyrrole moieties can thus be also produced (**6** in Fig. 8) and would also explain the presence of dominating component 3 in the mass spectrum (Fig. 5, Table 2). LDI mass spectrometry cannot distinguish between complex formation (**6**) and chemical bonding (**3**).

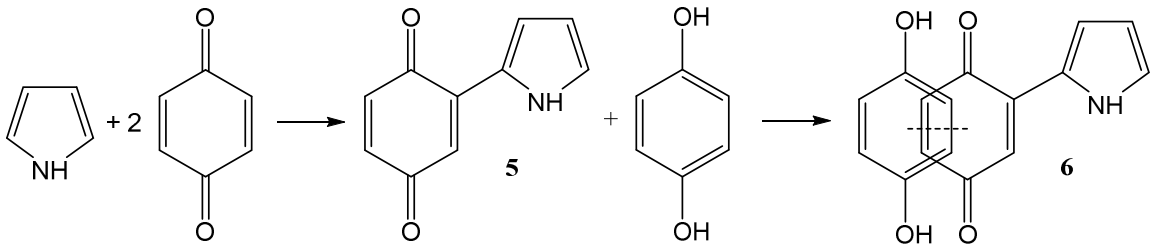

Fig. 8. An alternative route, when α-(*p*-benzoquinone)pyrrole (**5**) produces with hydroquinone a quinhydrone-like complex (**6**). Nitrogen atom in **6** can be protonated.

View Article Online
DOI: 10.1039/C8NJ01283K

Infrared spectra

Infrared spectrum of the product obtained in the absence of MSA (spectrum 0 M MSA in Fig. 9a) is very different from the spectrum of polypyrrole[2,29] as expected. We detect the bands of *p*-benzoquinone (spectrum *p*-BQ) and pyrrole (spectrum Py). The bands of quinhydrone (spectrum QH) and hydroquinone (spectrum HQ) are also found. This is supported by the presence of the band of OH stretching vibrations with a maximum at 3400 cm^{-1}. In addition, we observe a sharp band at 1407 cm^{-1}, which may correspond to the in-plane bending vibrations of hydroxyl group.

Infrared spectrum of the sample with the highest conductivity prepared in 0.1 M MSA (spectrum 0.1 M MSA in Fig. 9b), which has been analysed with mass spectrometry (Fig. 5, Table 1), is close to the infrared spectrum of quinhydrone (spectrum QH). Some peaks of *p*-benzoquinone (spectrum *p*-BQ) and of MSA counter-ion (Fig. 9c; spectrum NH_4MS) are also detected. The main bands of hydroquinone (spectrum HQ) and pyrrole (spectrum Py) are missing in the spectrum. The hypothesis of the compound composed of quinhydrone and pyrrole moieties (**6** in Fig. 8), eventually protonated with MSA, is supported by the infrared spectrum.

The infrared spectrum of the sample prepared in presence of 10 M MSA (Fig. 9c) is completely different, it is composed mainly of the bands of methanesulfonate (spectrum NH_4MS in Fig. 9c). In addition, we detect the band with maximum at 1607 cm^{-1} and the peaks at 1274 and 975 cm^{-1} associated probably with pyrrole, but the unambiguous assignment is not possible.

View Article Online
DOI: 10.1039/C8NJ01283K

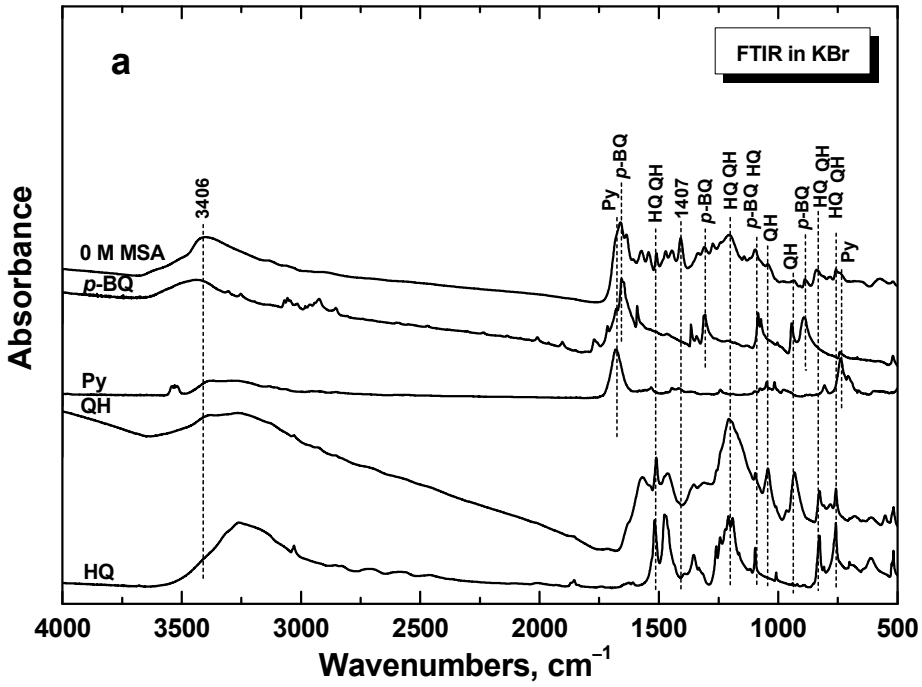

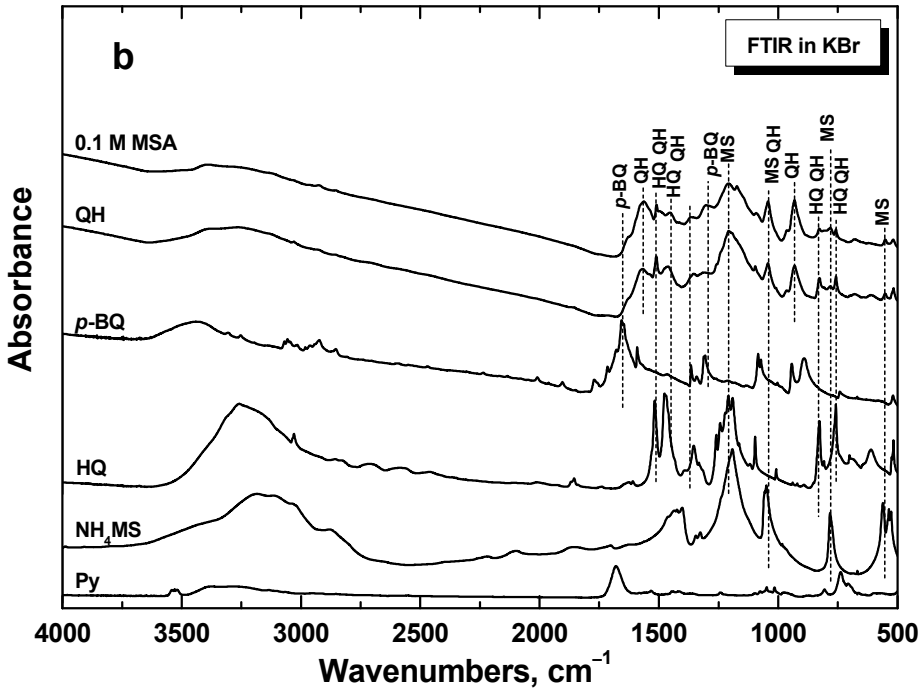

View Article Online
DOI: 10.1039/C8NJ01283K

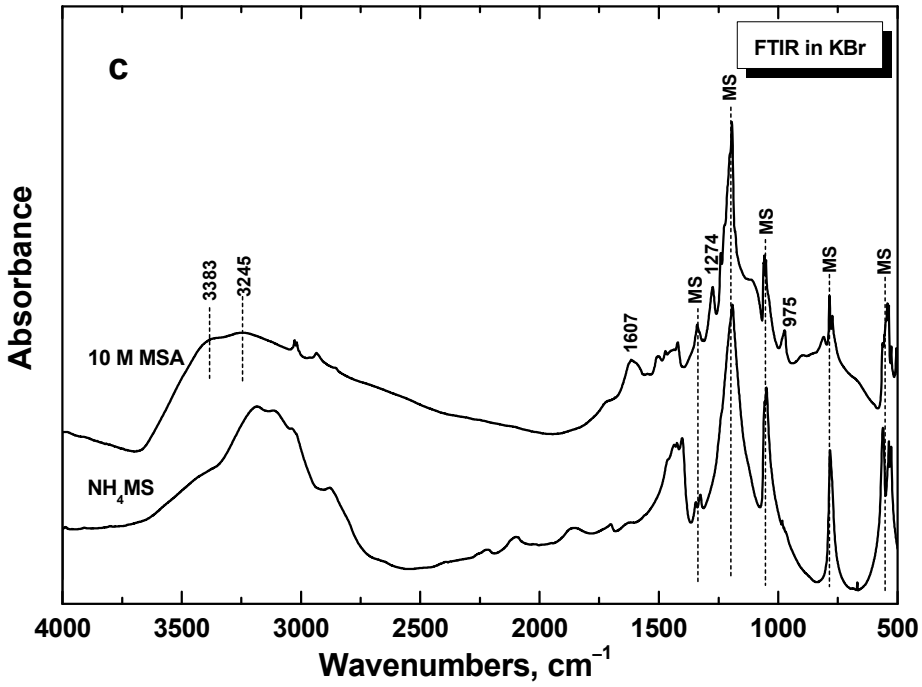

Fig. 9. FTIR spectra of the products of oxidation of pyrrole with *p*-benzoquinone (a) in absence of methanesulfonic acid, (b) in 0.1 M MSA (b) and (c) in 10 M MSA. Spectra of pyrrole (Py), *p*-benzoquinone (*p*-BQ), quinhydrone (QH), hydroquinone (HQ), and ammonium methanesulfonate (NH_4MS) are shown for comparison.

Raman spectra

Raman spectra recorded with 785 nm laser excitation are more sensitive to the pyrrole part of the samples. In the Raman spectrum of the non-conducting product obtained in the absence of MSA (spectrum 0 M MSA in Fig. 10a), we detect a strong fluorescence background corresponding to the presence of pyrrole (spectrum Py). The broad bands with the maxima corresponding to the main peaks of quinhydrone (spectrum QH) and *p*-benzoquinone (spectrum *p*-BQ) are observed in the spectrum. The main bands of the polypyrrole[29] (spectrum PPy G) are also present in the spectrum. This corresponds to the high sensitivity of the Raman spectra to the oxidized pyrrole on the surface.

The Raman spectrum of sample 0.1 M MSA with highest conductivity exhibits the main bands typical of pyrrole constitutional units in polypyrrole[29] (Fig. 10b; PPy) and some peaks of quinhydrone (spectrum QH). We also find the peaks of *p*-benzoquinone (spectrum *p*-BQ). The spectra are thus consistent with the expected chemistry (**6** in Fig. 8).

View Article Online
DOI: 10.1039/C8NJ01283K

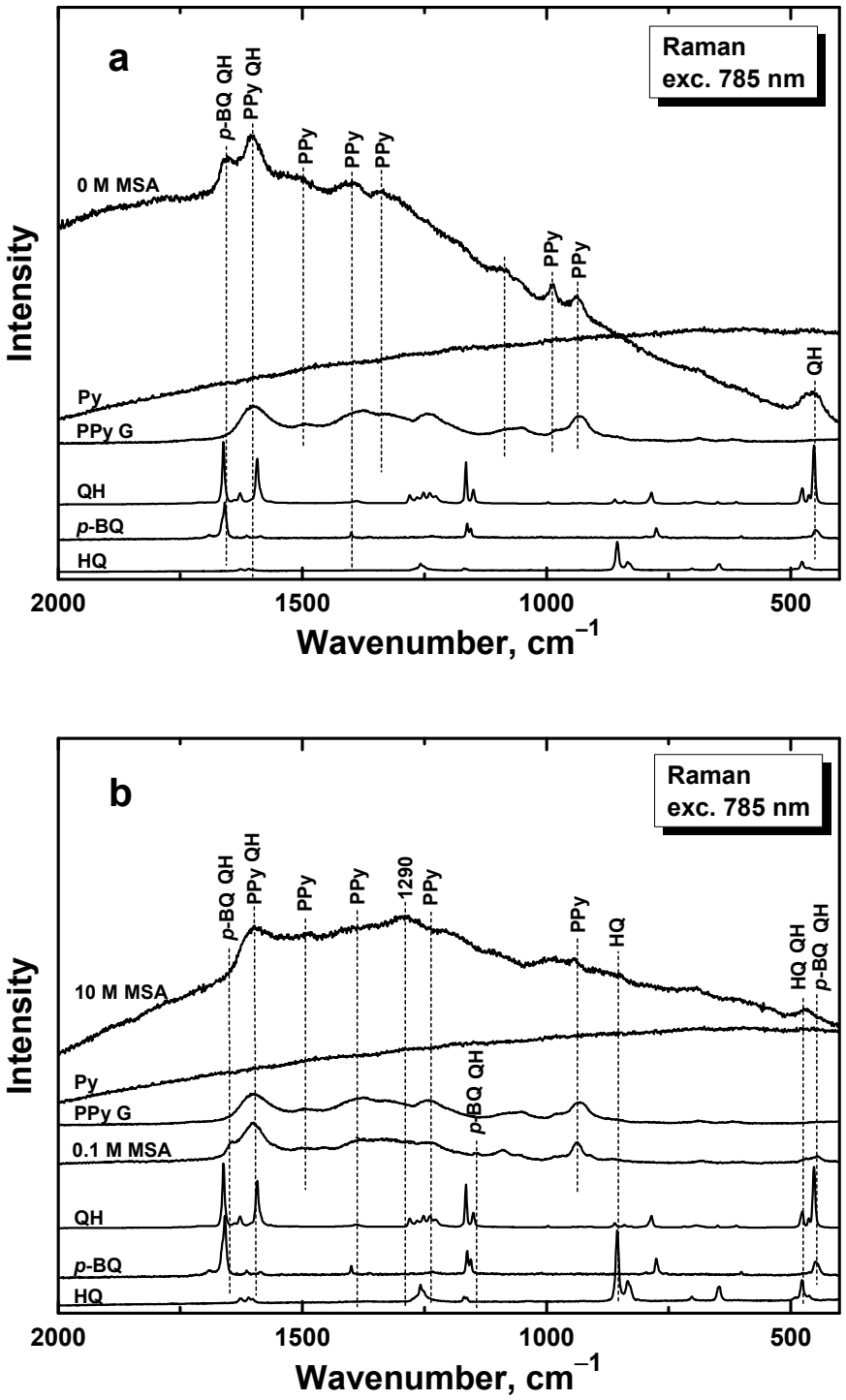

Fig. 10. Raman spectra of the products of oxidation of pyrrole with *p*-benzoquinone (a) in absence of methanesulfonic acid, and (b) 0.1 M MSA and 10 M MSA. The spectra of pyrrole (Py), *p*-benzoquinone (*p*-BQ), quinhydrone (QH), hydroquinone (HQ), ammonium methanesulfonate (NH_4MS) and of globular polypyrrole (PPy G) are shown for comparison.

View Article Online
DOI: 10.1039/C8NJ01283K

The Raman spectrum of the non-conducting sample prepared in 10 M MSA exhibits a strong fluorescence (Fig. 10b). In addition to the bands found in polypyrrole, it contains also broadened bands of quinhydrone (spectrum QH).

Electrorheology

The sample prepared in 0.1 M MSA with the highest conductivity, 1.4×10^{-5} S cm^{-1}, has subsequently been tested in electrorheology. Such conductivity is still low enough to avoid the current drifts that reduce the efficiency. The suspension behaved as a pseudoplastic fluid exhibiting typical shear-thinning behavior (Fig. 11). After application of an external electric field, however, shear stress increased by several orders of magnitude due to induced dipole–diplole interactions between the particles. Furthermore, the shear stresses at electric field strength 2 kV mm^{-1} were higher than those presented in the literature for similar electrorheological fluids based on conducting polymers[30–32] or respective oligomers.[10,33,34]

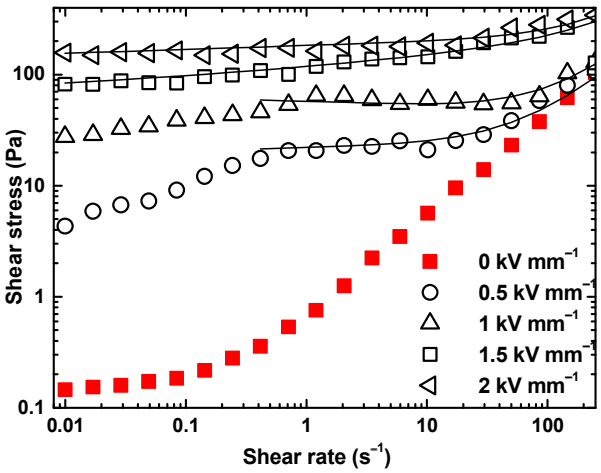

Fig. 11. Dependence of shear stress on the shear rate for the electrorheological fluid based on particles prepared in 0.1 M MSA at various electric field strengths. The particle concentration was 10 wt%. The solid lines represent fits of Cho-Choi-Jhon model.

In the state when electrostatic forces dominate over the hydrodynamic ones, yield stress as a function of external electric field strength follows the power law model, $\tau_y = k\, E^{\delta}$, where k reflects the rigidity of internal chain-like structures, E represents electric field strength and δ is exponential factor with values between 1.5 and 2, depending whether rigidity of the structures is directed mainly by conductivity or by polarization,[35,36] respectively. Therefore, the experimental data shown in Fig. 11 were fitted with corresponding model[37] in

View Article Online
DOI: 10.1039/C8NJ01283K

order to obtain the dynamic yield stress values. For the calculation of the dynamic yield stress in ER suspensions, the Bingham model (1) was frequently used at the beginning of 1990s:[38]

$$\tau = \tau_y + \eta_{pl} \times \dot{\gamma} \; ; |\tau| \geq \tau_y \quad (1)$$

$$\dot{\gamma} = 0; |\tau| < \tau_y$$

where τ stands for shear stress and η_{pl} is a plastic viscosity, or also modified Dougherty-Krieger model was used.[39] Since most of the suspensions do not exhibit a plateau at low shear rates, and rather display the local maximum or minimum, the Cho-Choi-Jhon model[40] (2) was developed:

$$\tau = \frac{\tau_y}{1+(t_1\dot{\gamma})^{\alpha}} + \eta_{\infty} \cdot \left(1 + \frac{1}{(t_2\dot{\gamma})^{\beta}}\right) \times \dot{\gamma} \quad (2)$$

In this model, the t_1 and t_2 are time constants inverse of the shear rate representing the region where the shear stress exhibits a minimum at a low shear rate, and inverse to a shear rate at which a pseudo-Newtonian behaviour starts, respectively. The exponent α is related to the decrease in the shear stress and the values of β vary between 0–1, since $d\tau/d\dot{\gamma} > 0$, and the η_{∞} represents shear viscosity at high shear rates.[40,41] After fitting experimental data with this model, the corresponding dynamic yield stresses were obtained together with rest of the model parameters (Table 3). In the case of measurements in electric field strengths 0.5 and 1 kV mm^{-1}, τ values increased slowly which is typical for diluted ER fluids in low electric field strengths. This region was not considered for fitting of the curves with the Cho-Choi-Jhon model.

Table 3. Parameters for the prepared ER fluid obtained from the Cho-Choi-Jhon model for various electric field strengths

Parameter	0.5 kV mm^{-1}	1 kV mm^{-1}	1.5 kV mm^{-1}	2 kV mm^{-1}
τ_y	13.8	46.5	81.0	106.9
t_1	0.010	0.016	0.009	0.001
α	0.50	0.31	0.04	0.52
η_{∞}	0.29	0.34	0.36	0.52
t_2	0.020	0.15	0.002	0.004
β	0.89	0.98	0.85	0.90

After the calculation of the yield stress τ_y from eq. 2 and applying power-law model, the value of parameter δ was found to be 1.50 which clearly indicates that the rigidity of the

View Article Online
DOI: 10.1039/C8NJ01283K

internal structures is driven mainly by conductivity mismatch between the particles and silicone oil.

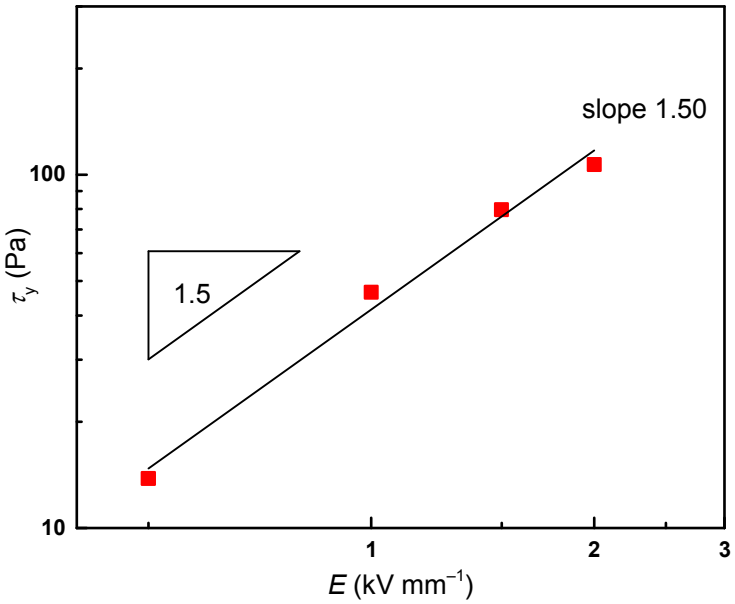

Fig. 12. Doublelogarithmic dependence of dynamic yield stress, τ_y, at 0.7 s^{-1} on the electric field strength, *E*.

The reproducibility of the electrorheogical behavior enabling a control over rheological parameters is important feature of the fluids. The present system reacts to the applied electric field promptly and after its removal the rheological parameters decrease again to the original off-field values (Fig. 13). Small variations in the on-field values can be attributed to the fact that the structures were formed during the shearing, which can lead to an uneven distribution of the created chains. Nevertheless, a capability of the prepared ER fluid to react promptly and reversibly to the applied electric field was confirmed.

View Article Online
DOI: 10.1039/C8NJ01283K

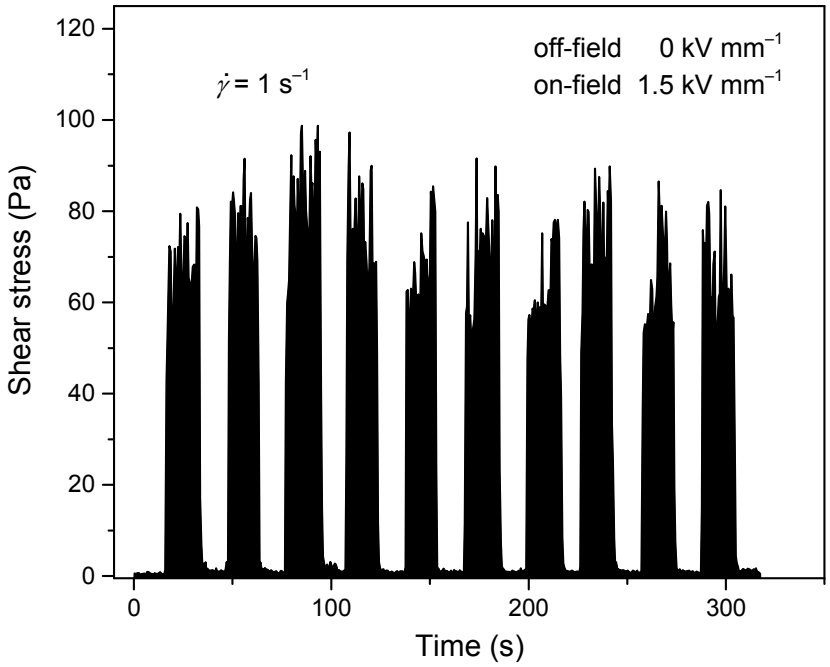

Fig. 13. Time-dependence of the shear stress on the presence of an electric field of strength 1.5 kV mm^{-1} and its absence at a shear rate of 1 s^{-1}.

Optical microscopy

Rheological investigations exhibit the presence of the yield stress upon application of the external electric field, indicating the development of the internal chain-like structures. The optical microscopy images were captured to demonstrate this fact (Fig. 14). The particles were randomly dispersed in silicone oil in the absence of the external electric field. After its application, however, the particles became polarized, orient perpendicularly to the electrodes, and create strands. Moreover, such structures are relatively robust and just partially branched, which indicates their enormous rigidity and toughness that have not been observed either for aniline oligomers or *p*-phenylenediamine analogues.[10,34]

View Article Online
DOI: 10.1039/C8NJ01283K

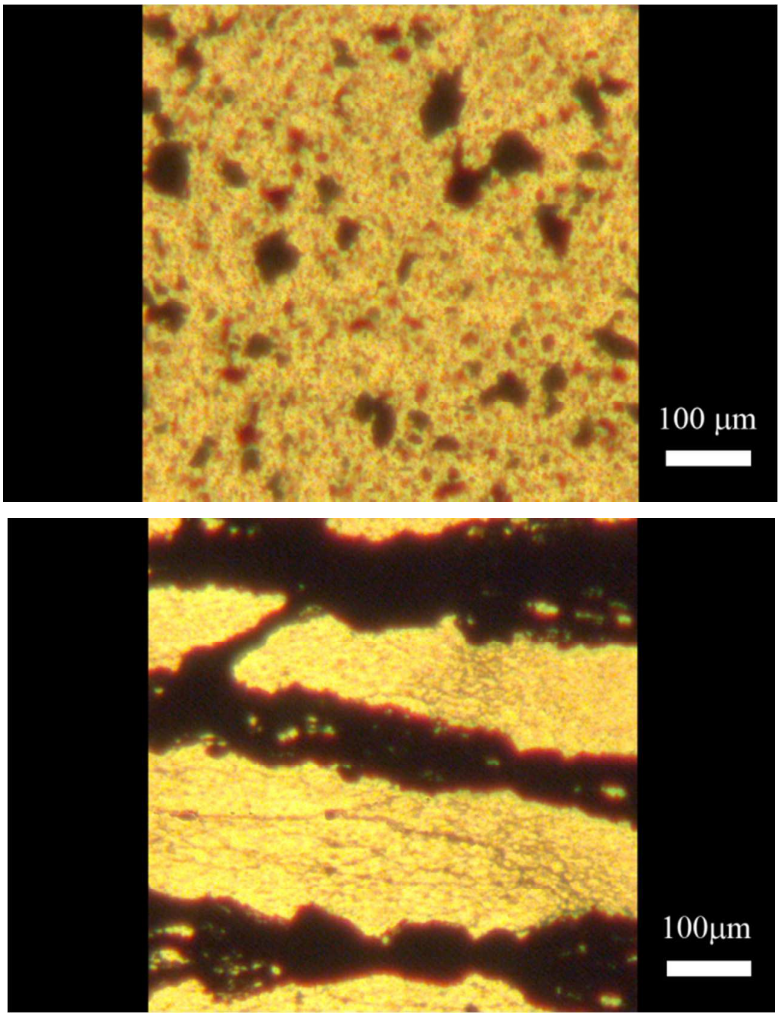

Fig. 14. Optical microscopy of 1 wt% suspension of pyrrole/*p*-benzoquinone adduct prepared in 0.1 M MSA and tested in the absence of an electric field (top) and at electric field strength 1 kV mm^{-1} (bottom).

Dielectric spectroscopy

Dielectric studies are frequently used as a complementary method for the evaluation of the dispersed phase suitability for application in electrorheology. Dielectric spectra were recorded and fit with H-N model to quantify the performance of prepared fluids based on pyrrole/*p*-benzoquinone adducts. It can be clearly seen that the relaxation process of interfacial polarization is shifted to the higher frequencies indicating relatively fast action at the interface (Fig. 15). The electrode polarization takes place at low frequencies as a very common phenomenon, which is also found in other electrorheological systems[42] and these data were excluded from the H-N model fitting.

View Article Online
DOI: 10.1039/C8NJ01283K

Basically there are two crucial parameters indicating the suitability of the material for application in electrorheology, such as dielectric relaxation strength, $\Delta\varepsilon'$, and relaxation time, t_{rel}. In the present case, the investigated sample possesses a high $\Delta\varepsilon' = 2.04$, which is considerably higher than those usually obtained for other semiconducting oligomers; in the case of aniline oligomers it was only[34] 0.75 and for oligomers of *p*-phenylenediamine[10] 1.85. The relaxation time is also extremely short, 8.6×10^{-6} s, and thus the response of the particles to the application of the external field is very fast and significantly faster than with aniline and *p*-phenylenediamine oligomers having 0.3 and 1.8 s, respectively. The very short t_{rel} fits well with the high conductivity of the particles[43] and further shifts the breakdown of the structures to much higher shear rates.[44]

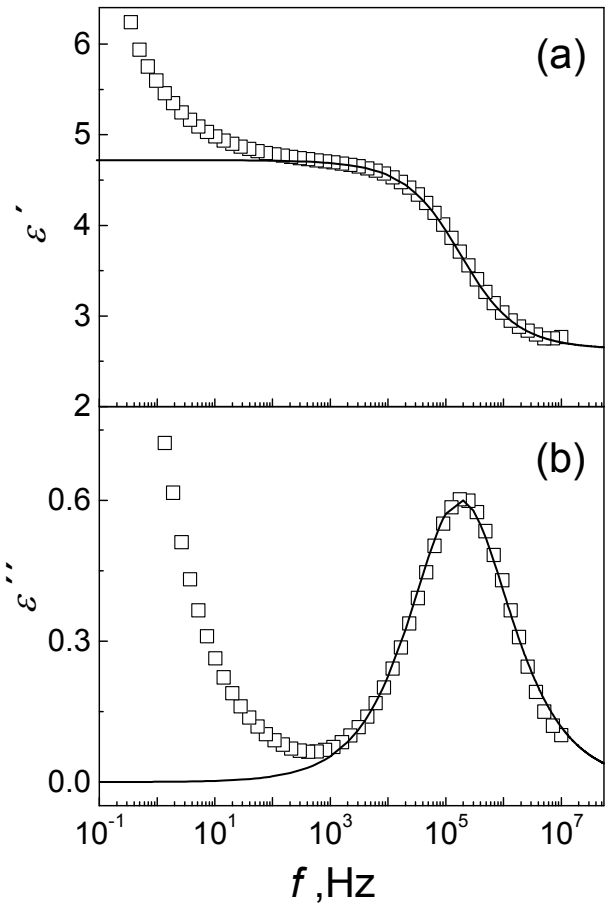

Fig. 15. The frequency dependence of (a) real part of relative permitivitty, ε', and (b) dielectric loss factor, ε'', and the fit of Havriliak-Negami model.

View Article Online
DOI: 10.1039/C8NJ01283K

Conclusions

The reaction between pyrrole and *p*-benzoquinone in acidic aqueous medium proceeded smoothly at room temperature to high yields. Low-molecular weight products were semiconducting and maximum conductivity was of the order 10^{-6} S cm^{-1} for the sample prepared in 0.1 M methanesulfonic acid. EPR spectra indicate the correlation between the conductivity and the concentrations of spins, i.e. the conductivity has electronic rather than ionic character. In water or at high acid content, only non-conducting products have been obtained. The FTIR and Raman spectroscopies indeed confirm that the molecular structure of the products considerably depends on the acidity condition in the reactions.

Only the product with the highest conductivity was analysed in detail. Mass spectrometry revealed that dominating compound was composed of one pyrrole and two *p*-benzoquinone/hydroquinone molecules, probably in quinhydrone complex. The oxidation to polypyrrole did not take place. The suitable level of conductivity makes pyrrole/*p*-benzoquinone adduct applicable in electrorheology. The fluid based on this adduct is very promising for its strong and fast responsive properties afforded by tough particle strands produced in electric field. This is in good agreement with the results obtained from both electrorheological investigations on a rotational rheometer as well as by optical microscopy and dielectric spectra. Due to the expected electroactivity, the prepared materials might also be suitable in the corrosion protection or as adsorbents, i.e. in applications that are typical of related oxidation products of pyrrole, viz. of polypyrrole.

Author information

Corresponding author

* (J.S.) E-mail: stejskal@imc.cas.cz

ORCID

Jaroslav Stejskal: 0000-0001-9350-9647

Miroslava Trchová: 0000-0001-6105-7578

Patrycja Bober: 0000-0002-1667-8604

Sergey Fillipov: 0000-0002-4253-5076

Miroslav Mrlik: 0000-0001-6203-6795

View Article Online
DOI: 10.1039/C8NJ01283K

Notes

The authors declare no conflict of interest.

Acknowledgment

The authors thank the Czech Science Foundation (17-04109S) for financial support. T.P. and M.M. also gratefully acknowledge the support of the Ministry of Education, Youth and Sports of the Czech Republic (NPU I, LO1504).

References

1 Omastová, M; Trchová, M; Kovářová, J; Stejskal J. Synthesis and structural study of polypyrroles prepared in the presence of surfactants. Synth. Met. 2003, 138, 447–455.

2 Stejskal, J.; Trchová, M. Conducting polypyrrole nanotubes: a review. Chem. Pap. 2018, 72; online. doi: s11696-018-0394x

3 Blinova, N. V.; Stejskal, J.; Trchová, M.; Prokeš, J.; Omastová, M. Polyaniline and polypyrrole: A comparative study of the preparation. Eur. Polym. J. 2007, 43, 2331–2341.

4 Chen, C. N.; Fu, X. W.; Fan, W.; Ma, T.; Wang, Z. B.; Miao, S. D. In-situ synthesis of core/shell structured polypyrrole/hydroquinone nano-beads. Mater. Lett. 2015, 138, 279–283.

5 Möhlau, R.; Redlich, A. Über die Kondensation von Parochinonen mit Indolen und Pyrrolen mit β-ständigem Wasserstoff. Ber. 1911, 44, 3605–3618.

6 Bullock, E. Addition of pyrroles to 1,4-benzoquinone. Can. J. Chem. 1958, 36, 1744.

7 Tandon, V. K.; Maurya, H. K. "On water": unprecendented nucleophilic substitution and addition reactions with 1,4-quinones in aqueous suspension. Tetrahedron Lett. 2009, 50, 5896–5902.

8 Stejskal, J.; Bober, P.; Trchová, M.; Horský, J.; Pilař, J.; Walterová, Z. The oxidation of aniline with p-benzoquinone and its impact on the preparation of the conducting polymer, polyaniline. Synth. Met. 2014, 192, 66–73.

9 Stejskal, J.; Trchová, M.; Morávková, Z.; Bober, P.; Bláha, M.; Pfleger, J.; Magdziarz, P.; Prokeš, J.; Havlicek, M.; Sariciftci, S.; Sperlich, A.; Dyakonov, V.; Zujovic, Z. Conducting materials prepared by the oxidation of p-phenylenediamine with p-benzoquinone. J. Solid State Electrochem. 2015, 19, 2653–2664.

View Article Online
DOI: 10.1039/C8NJ01283K

10 Plachy, T.; Sedlacik, M.; Pavlinek, V.; Stejskal, J. The observation of a conductivity threshold on the electrorheological effect of *p*-phenylenediamine oxidized with *p*-benzoquinone. J. Mater. Chem. C 2015, 3, 9973–9980.

11 Durgaryan. A. A.; Arakelyan, R. A.; Durgaryan, N. A. Synthesis of polymers containing polyaniline fragments linked by 1,4-benzoquinone groups. Russ. J. Gen. Chem. 2017, 87, 139–144.

12 Escolástico, C.; Santa María, M. D.; Claramunt, R. M.; Jimeno, M. L.; Alkorta, I.; Foces-Foces, C.; Cano, F. H.; Elguero J. Imidazole and benzimidazole addition to quinones. Formation of meso and d,l isomers and crystal structure of the d,l isomer of 2,3-bis(benzimidazol-1'-yl)-1,4-dihydroxybenzene. Tetrahedron 1994, 50, 12489–12510.

13 Kouno, K.; Ogawa, C.; Shimomura, Y.; Yano, H.; Ueda, Y. Interaction of imidazole derivatives with electron acceptors. II. Reaction products of imidazole with *p*-benzoquinone. Chem. Pharm. Bull. 1981, 29, 301–307.

14 Vaccaro, E.; Scola, D. A. New applications of polyaminoquinones. Chemtech 1999, 29, 15–23.

15 Grgur B. N. The role of aniline oligomers on the corrosion protection of mild steel. Synth. Met. 2014, 187, 57–60.

16 Abalyaeva, V. V.; Orlov, A. V.; Kiseleva, S. G.; Efimov, O. N.; Karpacheva, G. P. Electrochemical synthesis and study of poly(2,5-diarylamino-3,6-dichlorobenzoquinone) and its composite with multiwalled carbon nanotubes. Russ. J. Electrochem. 2017, 53, 210–216.

17 Melhi, S.; Ding, X. S.; Liu, Z. W.; Cao, C. X.; Han, B. H. A new strategy to microporous polypyrrole networks based on condensation of pyrrole and diketone. Macromol. Chem. Phys. 2016, 217, 1529–1533.

18 Emanuelsson, R.; Karlsson, C.; Huang, H.; Kosgei, C.; Stromme, M.; Sjödin, M. Quinone based conducting redox polymers for energy storage. Russ. J. Electrochem. 2017, 53, 8–15.

19 Choi, H. J.; Jhon, M. S. Electrorheology of polymers and nanocomposites. Soft Matter 2009, 5, 1562–1567.

20 Kwon, S. H.; Piao, S. H.; Choi, H. J. Electric field-responsive mesoporous suspensions: A review. Nanomaterials 2015, 5, 2249–2267.

21 Fang, F.; Choi, H. J.; Joo, J. J. Conducting polymer/clay nanocomposites and their applications. J. Nanosci. Nanotechnol. 2008, 8, 1559–1581.

View Article Online
DOI: 10.1039/C8NJ01283K

22 Liu, Y. D.; Choi, H. J. Electrorheological response of polyaniline and its hybrids. Chem. Pap. 2013, 67, 849–859.

23 Stejskal, J. Conducting polymer–silver composites. Chem. Pap. 2013, 67 814–848.

24 Rakić, A. A.; Vukomanović, M.; Trifunović, S.; Travas-Sejdic, J.; Chaudhary, O. J.; Horský, J.; Ćirić-Marjanović, G. Solvent effects on dopant-free pH-falling polymerization of aniline. Synth. Met. 2015, 209, 279–296.

25 Havriliak, S.; Negami, S. A complex plane representation of dielectric and mechanical relaxation processes in some polymers. Polymer 1967, 8, 161–210.

26 Sapurina I.; Li, Y.; Alekseeva, E.; Bober, P.; Trchová, M.; Morávková, Z.; Stejskal, J. Polypyrrole nanotubes: The tuning of morphology and conductivity. Polymer 2017, 113, 247–258.

27 Stejskal, J.; Sapurina, I.; Trchová, M.; Konyushenko, E. N. Oxidation of aniline: Polyaniline granules, nanotubes, and oligoaniline microspheres. Macromolecules 2008, 41, 3530–3536.

28 Bullock, E. The structure of pyrrole salts and the basic strengths of some simple pyrroles. Can. J. Chem. 1958, 36, 1686–1690.

29 Stejskal, J.; Trchová, M.; Bober, P.; Morávková, Z.; Kopecký, D.; Vrňata, M.; Prokeš, J.; Varga, M.; Watzlová, E. Polypyrrole salts and bases: Superior conductivity of nanotubes and their stability towards the loss of conductivity by deprotonation. RSC Adv. 2016, 6, 88382–88391.

30 Jun, C. S.; Kwon, S. H.; Choi, H. J.; Seo, Y. Polymeric nanoparticle-coated Pickering emulsion-synthesized conducting polyaniline hybrid particles and their electrorheological study. ACS Appl. Mater. Interfaces 2017, 9, 44811–44819.

31 Kim M. H.; Bae, D. H.; Choi, H. J.; Seo, Y. Synthesis of semiconducting poly(diphenylamine) particles and analysis of their electrorheological properties. Polymer 2017, 119, 40–49.

32 Lim, G. H.; Choi, H. J. Fabrication of self-assembled polyaniline tubes and their electrorheological characteristics. Colloids Surf. A, Physicochem. Eng. Asp. 2017, 530, 227–234.

33 Plachy, T.; Sedlacik, M.; Pavlinek, V.; Stejskal, J.; Graça, M. P.; Costa, L. C. Temperature-dependent electrorheological effect and its description with respect to dielectric spectra. J. Intel. Mater. Systems Struct. 2016, 27, 880–886.

34 Mrlik, M.; Sedlacik, M.; Pavlinek, V.; Bober, P.; Trchová, M.; Stejskal, J.; Saha, P. Electrorheology of aniline oligomers. Colloid Polym. Sci. 2013, 291, 2079–2086.

View Article Online
DOI: 10.1039/C8NJ01283K

35 Wu, C. W.; Conrad, H. A modified conduction model for the electrorheological effect. J. Phys. D, Appl. Phys. 1996, 29, 3147–3153.

36 Méheust, Y. The electrorheology of suspensions of Na-fluorhectorite clay in silicone oil. J. Rheol. 2011, 55, 809–833.

37 Kim, H. Y.; Choi, H. J. Core–shell structured poly(2-ethylaniline) coated crosslinked poly(methyl methacrylate) nanoparticles by graft polymerization and their electrorheology. RSC Adv. 2014, 4, 28511–28518.

38 Bonnecaze, R. T.; Brady, J. F. Yield stresses in electrorheological fluids. J. Rheol. 1992, 36, 73–115.

39 Goodwin, J. W.; Markham, G. M.; Vincent, B. Studies on model electrorheological fluids. J. Phys. Chem. B 1997, 101, 1961–1967.

40 Kim, S. G.; Lim, J. Y.; Sung, J. H.; Choi, H. J.; Seo, Y. Emulsion polymerized polyaniline sysnthesized with dodecylbenzenesulfonic acid and its electrorheological characteristics: Temperature effect. Polymer 2007, 48, 6622–6631.

41 Cho, M. S.; Choi, H. J.; Jhon, M. S. Shear stress analysis of a semiconducting polymer based electrorheological fluid system. Polymer 2005, 46, 11484–11488.

42 Stejskal, J.; Mrlík, M.; Plachý, T.; Trchová, M.; Kovářová, J. Li, Y. Molybdenum and tungsten disulfides surface-modified with a conducting polymer, polyaniline, for application in electrorheology. React. Funct. Polym. 2017, 120, 30–37.

43 Hao, T. Electrorheological suspensions. Adv. Colloid Interface Sci. 2002, 97, 1–35.

44 Wang, Z. Y.; Gong, Y. L.; Yang, F. Dielectric relaxation effect on flow behavior of electrorheological fluids. J. Intel. Mater. Systems Struct. 2015, 26, 1141–1149.

View Article Online
DOI: 10.1039/C8NJ01283K

Graphical abstract/Table of contents